Determination of Rotational Correlation Times from Deconvoluted Fluorescence Anisotropy Decay Curves. Demonstration with 6,7-Dimethyl-8-ribityllumazine and Lumazine Protein from *Photobacterium leiognathi* as Fluorescent Indicators†

Antonie J. W. G. Visser,*,‡ Taeke Ykema,‡ Arie van Hoek,§ Dennis J. O'Kane,∥ and John Lee∥

Departments of Biochemistry and Molecular Physics, Agricultural University, De Dreijen 11, 6703 BC Wageningen, The Netherlands, and Bioluminescence Laboratory, Department of Biochemistry, University of Georgia, Athens, Georgia 30602

Received March 5, 1984; Revised Manuscript Received August 10, 1984

ABSTRACT: The experimental and analytical protocols required for obtaining rotational correlation times of biological macromolecules from fluorescence anisotropy decay measurements are described. As an example, the lumazine protein from *Photobacterium leiognathi* was used. This stable protein (M_r 21 200) contains the noncovalently bound, natural fluorescent marker 6,7-dimethyl-8-ribityllumazine, which has in the bound state a long fluoresence lifetime (τ = 14 ns). Shortening of the fluorescence lifetime to 2.6 ns at room temperature was achieved by addition of the collisional fluorescence quencher potassium iodide. The shortening of τ had virtually no effect on the rotational correlation time of the lumazine protein (ϕ = 9.4 ns, 19 °C). The ability to measure biexponential anisotropy decay was tested by the addition of *Photobacterium* luciferase (M_r 80 000), which forms an equilibrium complex with lumazine protein. Under the experimental conditions used (2 °C) the biexponential anisotropy decay can best be described with correlation times of 20 and 60 ns, representing the uncomplexed and luciferase-associated lumazine proteins, respectively. The unbound 6,7-dimethyl-8-ribityllumazine itself (τ = 9 ns) was used as a model compound for determining correlation times in the picosecond time range. In the latter case rigorous deconvolution from the excitation profile was required to recover the correlation time, which was shorter (100–200 ps) than the measured laser excitation pulse width (500 ps).

Brownian rotation of fluorescent biopolymers can be directly followed via the time course of the polarized emission components after excitation with polarized light pulses. Information concerning rotational diffusion of macromolecules has been reviewed in the last two decades (Tao, 1969; Yguerabide, 1972; Rigler & Ehrenberg, 1973; Wahl, 1983).

The method in which polarized fluorescence is created by a short pulse of polarized light is a relaxation method. It measures the return to randomization of a previously created, anisotropic distribution of fluorescent molecules. The time constant of this process (the rotational correlation time) is proportional to the size of the fluorescent particle. The time dependence of the fluorescence anisotropy is related to the fluorescence intensity polarized parallel [$\parallel(t)$] and perpendicular [$\perp(t)$] to the polarized excitation light:

$$r(t) = [\parallel(t) - \perp(t)]/[\parallel(t) + 2\perp(t)] \quad (1)$$

The experimentally measurable quantity $r(t)$ is also proportional to the autocorrelation function for the dipole reorientation angle (Fleming et al., 1976):

$$r(t) = \tfrac{2}{5}\langle P_2[\mathbf{e}(0)\cdot\mathbf{e}(t)]\rangle = \tfrac{2}{5}[\tfrac{3}{2}\langle\cos^2\omega(t)\rangle - \tfrac{1}{2}] \quad (2)$$

P_2 is the second Legendre polynomial of the dipole reorientation angle ω at time t, $\mathbf{e}$ being unit vectors along the transition dipole at $t = 0$ or $t = t$, respectively. In eq 2 we assume that absorption and emission vectors coincide. In principle, the expression for $\langle P_2\rangle$ is dependent on the shape of the molecule. In many examples, however, $\langle P_2\rangle$ will decay according to a spherical rotor, i.e.

$$\langle P_2[\mathbf{e}(0)\cdot\mathbf{e}(t)]\rangle = \exp(-t/\phi) \quad (3)$$

where ϕ is $1/(6D)$, D being the rotational diffusion coefficient with $D = kT/(6V\eta)$, k is the Boltzmann constant, η is the solvent viscosity, V is the molecular volume, and T is the absolute temperature. For nonspherical molecules the time dependence of the anisotropy is more complex, and anisotropic rotation gives rise to five exponential terms for an irregularly shaped body (Belford et al., 1972). In practical cases it can be shown from numerical analysis that at most three exponential terms can be distinguished (Small & Isenberg, 1977). Ellipsoids of revolution contain three exponential terms (Tao, 1969). In practice, however, three-component anisotropy decays have never been observed. Evidence for the existence of anisotropic rotation has been provided recently from time-resolved fluorescence anisotropy measurements using three different fluorescent lipid molecules that were noncovalently attached to a specific lipid transport protein (Berkhout et al., 1984). In the three different cases the anisotropy decayed according to a single exponential decay law, but the correlation times were widely different. Apart from rotational motion of spherical and nonspherical rotors, fluorescence anisotropy decay has also been applied to investigate segmental flexibility in proteins and nucleic acids. Among the many available examples we want to mention the flexibility in an antibody molecule (Yguerabide et al., 1970), the flexibility of hinged macromolecules in general (Harvey & Cheung, 1980), and the torsional dynamics of DNA (Thomas et al., 1980). Finally, fluorescence anisotropy decay of fluorophores embedded in artificial bilayer membranes has been extensively

† This work was supported by the Netherlands Foundation for Chemical Research (S.O.N), with financial aid from the Netherlands Organization for the Advancement of Pure Research (Z.W.O), National Institutes of Health Grant GM28139, and NATO Grant 835/83.

‡ Department of Biochemistry, Agricultural University.
§ Department of Molecular Physics, Agricultural University.
∥ University of Georgia.

0006-2960/85/0424-1489$01.50/0

considered [see, for example, Kinosita et al. (1977), Heyn (1979), Lipari & Szabo (1980), Kinosita et al. (1982), and Dale (1983)].

The method has two main limitations. First, the time scale of observation of rotational motion is dictated by the average fluorescence lifetime (τ) of the probe (in the order of one to tens of nanoseconds) and is therefore limited to the subnanosecond–submicrosecond time regime. Second, especially manifest in the investigation of subnanosecond rotational motion, the experimental data need to be deconvoluted to obtain correlation times that are not perturbed by instrumental distortions due to the finite excitation pulse width.

For the technique of time-correlated single-photon counting Wahl (1977) has derived the statistical errors in the correlation times as a function of fluorescence lifetimes. It was demonstrated that maximally a 10% error in correlation times is involved for ϕ between 0.1τ and 100τ. Wahl (1979) also described an algorithm based on the nonlinear least-squares procedure, which was demonstrated with simulated data using an experimental exciting pulse from a discharge lamp. From a pure simulation study Papenhuyzen & Visser (1983) have shown that when both τ and ϕ are of the same magnitude as the stimulating pulse width, deconvolution from the pump function is required to retrieve precise rotational correlation times. This problem was already advanced by Munro et al. (1979), but no details were presented in that study.

We have considered these aspects in more detail by emphasizing both experimental and analytical features connected with anisotropy decay. For test purposes an appropriate, well-behaved fluorescent protein was used. While most biochemical fluorescent systems studied thus far are hampered by the fact that the fluorescence decay is nonexponential, our system has the advantage that the fluorescence decays in a strictly exponential fashion and that the fluorescence yield is very high ($Q = 0.6$).[1] The protein has a M_r of 20 000 and contains 6,7-dimethyl-8-ribityllumazine as a noncovalently bound prosthetic group. The chromophoric system and the properties of this lumazine protein, which has a function in bacterial bioluminescence, have been sufficiently described in the literature (Visser & Lee, 1980, 1982; Lee, 1982; Vervoort et al., 1983; Lee et al., 1985; O'Kane & Lee, 1985a,b; O'Kane et al., 1985). The chromophore free from the protein is characterized by a rotational correlation time much shorter than the measured laser pulse width (500 ps) and therefore constitutes a challenging object for the recovery of picosecond correlation times.

Materials and Methods

The lumazine protein from *Photobacterium leiognathi* strain A2D, luciferase from *Photobacterium phosphoreum* strain A13, and the authentic ligand 6,7-dimethyl-8-ribityllumazine were obtained as previously described (Small et al., 1980; O'Kane et al., 1985; Lee, 1982). The solutions were buffered with 50 mM sodium phosphate containing 5 mM 2-mercaptoethanol and were at pH 7.0. Other chemicals were of the best commercial grade.

Experimental Setup. The apparatus used was as previously described (Visser & van Hoek, 1979, 1981) with the addition of the pulse picker of van Hoek & Visser (1981). The light source was the 457.9-nm line from a mode-locked Ar ion laser, and for selection of polarized emission we used a fast-rotating (<0.3 s for 90°) magnet-driven sheet-type polarizer with a 38-mm aperture (Polaroid Type HN38) that provided a high optical throughput. In the practical experiment using 0.1–10 μM solutions the 0.4-nJ (van Hoek & Visser, 1983) pulses of excitation were attenuated by a factor of 200–5000 by using neutral density filters. The frequency of detected photons was held at 15 kHz, i.e., 5% of the rate of the excitation photons, to prevent pulse pileup (Harris & Selinger, 1979).

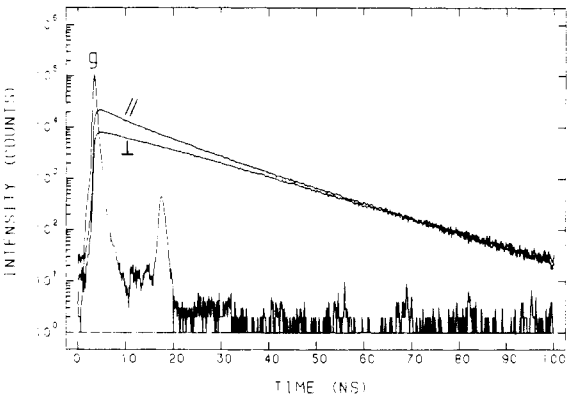

FIGURE 1: Measured excitation profile (g) and fluorescence intensity components ($\parallel$ and $\perp$) of lumazine protein from *P. leiognathi* (7.7 μM in 0.1 M potassium phosphate, pH 7.0) at 2 °C. From the 1024 data points available for each curve, the first 823 were used for the plot to yield a time span of 100 ns. The curves were plotted in a semilogarithmic way to emphasize the afterpulse in the excitation response function. The perpendicular component ($\perp$) has been multipled by 0.95 (factor b in eq 4 and 5) to obtain optimum tail matching. All curves have been divided by a so-called correction curve to remove electronic distortions (cf. Materials and Methods).

At very low concentration of fluorescent material care has to be taken of emission arising from impurities in sample and buffer. As a routine procedure we always took data from a sample without the implemented chromophore. Since the optical density of the fluorescent compound at the wavelength of excitation was mostly smaller than 0.05, background data were directly subtracted from fluorescence data.

In the experimental data sometimes an oscillation-like distortion could be observed. The method used to remove these "residual" distortions was to divide the experimental data by a so-called "correction curve" (Haehnel et al., 1982; Turko et al., 1983; Searle et al., 1983). With the experimental setup similar to the operational conditions except that the shutter in front of the laser output is closed, the photomultiplier is detecting photons of (uncorrelated) room light at the same 15-kHz photon frequency. In principle, the response in the MCA should be a straight line, but the oscillation-like distortions are superimposed. This curve can be used to correct by division similar distortions in the decay profiles of the polarized emission components.

In order to demonstrate the performance of the system, plots of the measured laser pulse profile and polarized fluorescence components are shown in Figure 1 on a semilogarithmic scale. From the polarized intensity components the total fluorescence $[\parallel(t) + 2\perp(t)]$ and fluorescence difference $[\parallel(t) - \perp(t)]$ curves can be constructed (cf. below). The laser pulse at 457.9 nm has a measured full width at half-maximum of 0.5 ns, longer than the nominal value around 80 ps. Also noteworthy in the semilogarithmic plot of Figure 1 is the afterpulse at around 13 ns after the main pulse maximum, the latter having a 300-fold higher intensity.

Data Analysis. Initially one constructs from the experimental $\parallel(t)$ and $\perp(t)$

$$d^{\text{exptl}}(t) = \parallel(t) - b\perp(t) \quad (4)$$

$$s^{\text{exptl}}(t) = \parallel(t) + 2b\perp(t) \quad (5)$$

[1] Abbreviations: Q, fluorescence quantum yield; MCA, multichannel analyzer; TAC, time to amplitude converter.

The instrumental correction factor b was determined as described earlier and was usually equal to 1 (Visser & van Hoek, 1979). Because of the involvement of the excitation pulse $g(t)$ the following convolution product should be considered:

$$s^{\text{calcd}}(t) = g(t)*S(t) \tag{6}$$

$$S(t) = \sum_{i=1}^{n} \alpha_i \exp(-t/\tau_i) \tag{7}$$

τ_i is the fluorescence lifetime of component i. The excitation pulse is taken into account by representing it by a local binomial, which is sufficiently accurate when the pulse is a smooth curve [see Wahl (1979) for an elaboration of this idea]. In the case of rotational homogeneity, i.e., all the contributing chromophores have similar rotational movements (Dale et al., 1977), we have

$$R(t) = \sum_{j=1}^{m} \beta_j \exp(-t/\theta_j) \tag{8}$$

$$D(t) = S(t)\, R(t) \tag{9}$$

$$d^{\text{calcd}}(t) = s^{\text{calcd}}(t)\, R(t) \tag{10}$$

θ_j is the rotational correlation time of component j. For the fluorescence and anisotropy decay analysis we constructed a set of flexible, interactive Fortran programs, which run on a DEC-10 mainframe computer. It consists of a data preparation/manipulation program and a fluorescence/anisotropy decay program.

For the determination of the time constants and relative amplitudes a nonlinear least-squares method was used, based on a variant of the well-known Marquardt algorithm [Marquardt, 1963; Grinvald & Steinberg, 1974; see McKinnon et al. (1977) and O'Connor et al. (1979) for comparison of methods]. This algorithm is convenient because one can make use of the structure of the data by giving the content in each data channel k a weighting factor w that is related to the inverse of the estimated standard deviation for the content. For fluorescence decay the weighting factor is related to $1/s^{\text{exptl}}$ in each data channel; for anisotropy decay weighting factors as derived by Wahl (1979) were used. With the nonlinear least-squares algorithm, parameters describing fluorescence and anisotropy decay models are optimized in an iterative procedure until χ^2 has been minimized (only presented for fluorescence decay).

$$\chi^2 = \frac{\sum_{k=n_1}^{n_2} w_k (s_k^{\text{exptl}} - s_k^{\text{calcd}})^2}{n_2 - n_1 - n_t + 1} \tag{11}$$

n_t = total number of parameters (α_i, τ_i) or (β_i, ϕ_i). Both $g(t)$ and $s^{\text{exptl}}(t)$ were normalized to their maximum values; the weighting factors were normalized such that

$$\sum_{k=n_1}^{n_2} w_k = N$$

with N the total number of channels used. Apart from the optimized parameters with respect to χ^2, confidence limits and the standard deviations for them are derived. In addition to this, the programs keep track of the Durbin–Watson value (Lampert et al., 1983):

$$\text{DW} = \frac{\sum_{k=n_1+1}^{n_2} [w_k(s_k^{\text{exptl}} - s_k^{\text{calcd}}) - w_{k-1}(s_{k-1}^{\text{exptl}} - s_{k-1}^{\text{calcd}})]^2}{\sum_{k=n_1}^{n_2} w_k (s_k^{\text{exptl}} - s_k^{\text{calcd}})^2} \tag{12}$$

This parameter gives a measure of the correlation between the residual values in neighboring channels. The Durbin–Watson parameter has recently been used as a "goodness of fit" criterion in fluorescence decay analysis of standard compounds (Lampert et al., 1983).

An empirical procedure has been developed, which turned out to be very useful, especially in heterogeneous decay, to investigate whether χ^2 is a real operating minimum for the set of optimized parameters. A 2% increase in one parameter value is introduced and the corresponding higher χ^2 value calculated. By parabolic extrapolation the parameter value upon a 5% increase in χ^2 is determined. The same is done for a 2% decrease in that particular parameter value. If the spread in parameter value is symmetrical, χ^2 is an operating minimum. The whole procedure is then successively repeated for the other parameters. The relative changes of 2% and 5% are arbitrarily chosen, and they are satisfactory in practice. It should be emphasized that the procedure has an empirical not a statistical basis.

Results

Long Correlation Time and Long Fluorescence Lifetime. The experimental and calculated time-dependent emissions given in Figure 2 show that the fluorescence of lumazine protein decays monoexponentially. A plot of the weighted residuals fluctuating around the base line (top panel, Figure 2A) corroborates this point. The lifetime, experimental details, and statistical information, also from other experiments, are given in Table I.

As demonstrated in Figure 2B, the decay of the emission anisotropy gives rise to a single correlation time of 18 ns (Table I). The initial anisotropy (at t = 0 ns) is high, implicating tight binding of the chromophore. In this particular case the afterpulse is canceled in part. In fact, for this experiment no deconvolution is required to retrieve the correct parameters (Visser & Lee, 1982). The deviation function of the weighted residuals fluctuates around the base line, and the larger amplitudes in the early time channels account for the fact that the anisotropy is weighted in proportion to the fluorescence intensity in that particular channel.

Long Correlation Time and Short Fluorescence Lifetime. Binding of the lumazine derivative to its apoprotein is stronger at higher ionic strength of the solution (Visser & Lee, 1980). Considering the exposure of the bound lumazine to the aqueous solvent, one might expect no other effects of iodide than to quench the lumazine fluorescence dynamically. The quenched fluorescence by KI also decays exponentially but with a shorter single lifetime [cf. Lee et al. (1985)]. Results are collected in Table I.

The anisotropy can be analyzed only from the initial part of the decay as demonstrated in parts A and B of Figure 3 for two temperatures. The afterpulse is very pronounced now, and proper deconvolution of the data takes this effect into account. It is clear from Figure 3 that the afterpulse creates new polarization events and should be considered as an echo of the response to the main excitation pulse. If the anisotropy is not deconvoluted, the afterpulse remains invisible. The noise becomes very large at longer times because the fluorescence diminishes rapidly. To prevent the noise exploding out of scale, the experimental data were cut off at r = 0.4 and 0.0. Also a digital filter was applied. We obtained the same correlation times as for the unquenched lumazine protein (Table I).

Hetereogeneity of Anisotropy Decay in the Case of Protein–Protein Association. As demonstrated previously by Visser & Lee (1982), lumazine protein can associate with luciferase to form a protein complex of total M_r 100 000, thus

Table I: Parameters Describing Fluorescence and Anisotropy Decay of Free and Bound 6,7-Dimethyl-8-ribityllumazine

sample	peak ch pulse[a]	peak ch F[b]	no. of ch	ns/ch	n_1	n_2	τ (ns)	β	ϕ (ns)	DW	χ^2
7.7 μM lumazine protein, 2 °C	29	41	1024	0.122	30	823	15.1			1.38	2×10^{-6}
					30	530		0.382	18.1	1.80	7×10^{-4}
7.7 μM lumazine protein + 250 mM KI, 4 °C	21	24	512	0.187	21	256	3.6			0.18	4×10^{-6}
					21	221		0.339	16.2	1.93	8×10^{-4}
7.7 μM lumazine protein, 19 °C	21	28	512	0.187	21	512	14.3			0.10	5×10^{-5}
					21	421		0.364	9.4	1.40	8×10^{-4}
7.7 μM lumazine protein + 250 mM KI, 19 °C	20	24	512	0.187	21	256	2.6			0.21	2×10^{-6}
					21	221		0.320	9.3	1.89	8×10^{-4}
57 μM lumazine, 3 °C	81	131	1024	0.0262	81	512	9.0			1.20	5×10^{-5}
					70	150		0.184	0.157	1.89	6×10^{-3}
57 μM lumazine + 238 mM KI, 3 °C	79	94	1024	0.0262	81	512	0.86			0.20	1×10^{-5}
					70	150		0.205	0.135	1.71	4×10^{-3}
57 μM lumazine, 19 °C	88	131	1024	0.0262	81	512	8.3			0.64	6×10^{-5}
					70	150		0.128	0.083	1.94	8×10^{-3}
57 μM lumazine + 238 mM KI, 19 °C	82	94	1024	0.0262	81	512	0.59			0.06	3×10^{-5}
					70	150		0.161	0.067	1.49	2×10^{-3}

[a] ch = channel. [b] F = fluorescence.

Table II: Association between Lumazine Protein and Luciferase[a]

β_1	$-\Delta\phi_1$ (ns)	ϕ_1 (ns)	$+\Delta\phi_1$ (ns)	β_2	$-\Delta\phi_2$ (ns)	ϕ_2 (ns)	$+\Delta\phi_2$ (ns)	DW	$\chi^2 \times 10^4$	remarks
0.378	0.8	28.8	0.8					1.68	5.48	*b*
0.050	1.1	6.8	1.9	0.328	1.1	33.4	0.9	1.90	4.87	*c*
0.290	0.5	20.0	0.8	0.088	17.0	120.0	14.2	1.79	5.18	*d*
0.289	0.5	20.0	0.8	0.089	16.5	115.0	13.4	1.80	5.17	*d*
0.287	0.5	20.0	0.8	0.091	16.5	110.0	12.6	1.80	5.16	*d*
0.286	0.5	20.0	0.8	0.093	16.2	105.0	11.8	1.81	5.14	*d*
0.284	0.5	20.0	0.7	0.095	18.8	100.0	10.6	1.81	5.13	*d*
0.281	0.5	20.0	0.7	0.097	16.5	95.0	10.4	1.82	5.11	*d*
0.279	0.6	20.0	0.7	0.100	18.5	90.0	9.6	1.82	5.10	*d*
0.276	0.6	20.0	0.7	0.102	31.3	85.0	8.7	1.83	5.08	*d*
0.272	0.6	20.0	0.7	0.106	36.9	80.0	8.1	1.83	5.07	*d*
0.268	0.6	20.0	0.7	0.110	18.9	75.0	7.8	1.84	5.05	*d*
0.263	0.6	20.0	0.7	0.115	12.7	70.0	7.2	1.84	5.04	*d*
0.257	0.7	20.0	0.7	0.121	8.1	65.0	6.3	1.85	5.03	*d*
0.250	0.7	20.0	0.7	0.129	6.0	60.0	5.9	1.85	5.02	*d*
0.240	0.8	20.0	0.7	0.139	4.6	55.0	5.0	1.85	5.02	*d*
0.227	0.8	20.0	0.7	0.151	3.4	50.0	4.3	1.84	5.03	*d*
0.208	1.0	20.0	0.8	0.170	2.6	45.0	3.5	1.83	5.06	*d*
0.181	1.2	20.0	0.9	0.197	1.8	40.0	3.0	1.81	5.13	*d*
0.135	2.6	20.0	1.1	0.244	1.3	35.0	1.8	1.77	5.24	*d*
0.044	3.9	20.0	2.8	0.335	0.8	30.0	1.1	1.70	5.44	*d*
0.008	1.9	20.0	1.9	0.370	0.3	25.0	0.4	0.96	9.53	*d*
0.189	0.4	20.0	0.4	0.189	0.4	20.0	0.4	0.27	33.25	*d*
0.320	0.3	20.0	0.3	0.058	0.6	15.0	0.6	0.22	40.50	*d*
0.364	0.3	20.0	0.3	0.014	1.0	10.0	1.0	0.24	36.82	*d*

[a] Experimental details are the following: 7.5 μM lumazine protein, 62 μM luciferase, 1 M potassium phosphate, pH 7.0, 2 °C; no. of channels = 512, excitation maximum in channel 32, emission maximum in channel 41, ns/channel = 0.1172, analysis always from channel 38 (n_1) to channel 512 (n_2). The fluorescence lifetime τ = 14.58 ns. The initial anisotropy was kept constant at $\beta_1 + \beta_2 = 0.378$; $\pm\Delta\phi$ are the upper and lower parameter limits upon a 5% change in χ^2. Further details are given under Data Analysis. [b] Single exponential analysis. [c] All parameters free. [d] ϕ_1 and ϕ_2 fixed.

a much larger rotating particle. The dissociation constant can be affected by varying the solution conditions like ionic strength and temperature. The system is very well-behaved as judged from the anisotropy decay in Figure 4. A nonlinear least-squares analysis should directly yield the expected correlation times of 20 and 60 ns, characteristic for free and complexed lumazine proteins, respectively (2 °C). Since the fluorescence yield does not change in the protein complex, the preexponential factors are direct measures of the species concentrations in the equilibrium.

The experimental data presented in Figure 4 are very good test data to see how far apart the correlation times must be for separate determination. A similar problem regarding fluorescence lifetimes was investigated earlier (Gafni et al., 1975). We have fixed one correlation time and varied the other one systematically while treating the amplitudes as free parameters. The data in Table II are interesting, because the results are not realistic if the parameters are adjusted to values that correspond to a minimum χ^2 and a maximum Durbin–Watson parameter. The correlation time is far too short in this particular case. Note also that there is an asymmetrical spread in the upper and lower values of the parameters on a 5% change in χ^2. From inspection of Table II we arrive at the conclusion that the correlation times of 20 and 60 ns are associated with both a symmetrical spread, a minimum χ^2, and a maximum Durbin–Watson parameter.

In this particular example the range where good fitting criteria are obtained is very broad. The multitude of possible solutions is caused by several factors. The contribution of the long component is smaller than that of the shorter component, so that the longer one is predominant in the noisy tail of the curve. Furthermore, the anisotropy extends only over 55 ns, implying that the depolarization is not complete. It is clear from the data in Table II that the fit becomes worse as the variable correlation time approaches the shorter one. The change in parameter values for a 5% change in χ^2 is in this respect very illustrative (cf. Data Analysis). The optimized fit of 20 and 60 ns simultaneously corresponds to a symmetrical

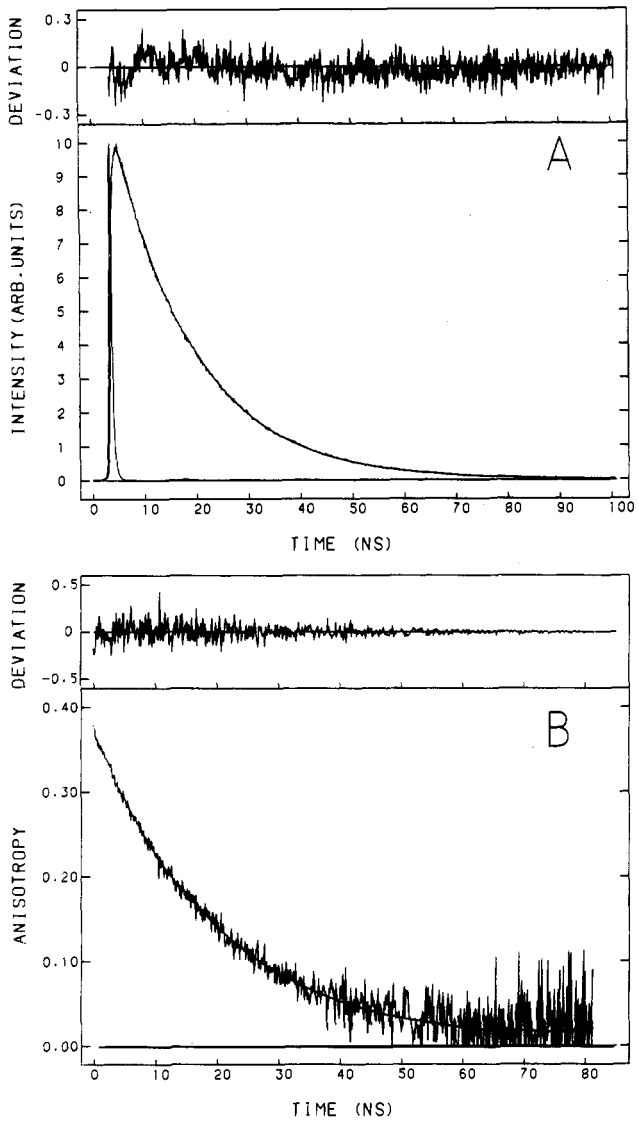

FIGURE 2: Fluorescence (A) and anisotropy (B) decay analysis of 7.7 μM lumazine protein from *P. leiognathi* at 2 °C. Experimental curves $s^{expt}(t)$ and $r^{expt}(t)$ were constructed from component curves $\parallel(t)$ and $\perp(t)$ of Figure 1 (cf. Data Analysis). Calculated response curves are also given, together with the deviation of the experimental response from single exponential functions in each data channel k: $DV_k = w_k RES_k$, where w_k is a weighting factor (see Data Analysis) and RES_k is the difference between the experimental and calculated value in channel k. Parameter values are τ = 15.1 ns and ϕ = 18.1 ns. These values and additional experimental details are given in Table I.

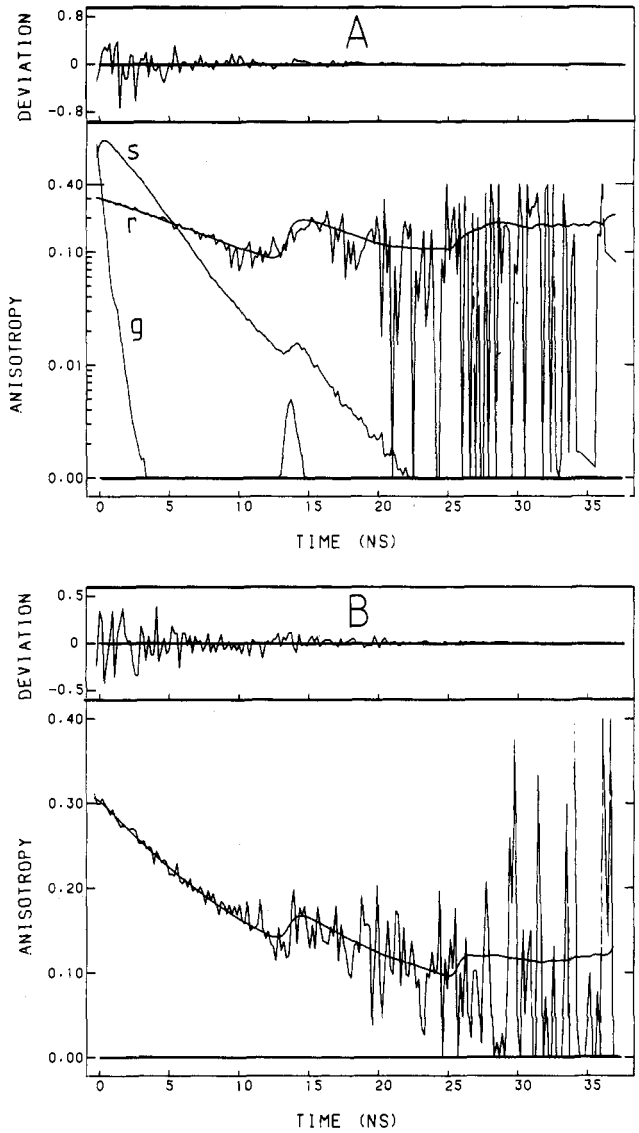

FIGURE 3: Anisotropy decay analysis of 7.7 μM lumazine protein from *P. leiognathi* in the presence of 250 mM collisional quencher KI. In (A) the excitation pulse and total fluorescence have been incorporated (both scaled to 1.0) in a semilogarithmic plot to show that the afterpulse becomes significant as the fluorescence lifetime is reduced from 15 (unquenched) to 2.6 ns (quenched) at 19 °C. In (B) the decay analysis is presented for a temperature of 4 °C. The recovered correlation times are unaffected by the shortening of the lifetimes. Parameter values are as follows: at 20 °C, τ = 2.6 ns and ϕ = 9.4 ns; at 4 °C, τ = 3.6 ns and ϕ = 16.2 ns. See Table I for additional information.

distribution of upper and lower bound values upon the 5% change in χ^2. The spread in amplitudes is always symmetrical and has been omitted in Table II.

Picoseond Correlation Times. The broadening of the laser pulse implies that picosecond correlation times can only be obtained after rigorous deconvolution of the time-dependent anisotropy from the excitation pulse. The free lumazine derivative itself is a good model compound to establish the limit of shortest measurable correlation times. Free lumazine has a high quantum yield of fluorescence (Q = 0.45) and long lifetime of the fluorescence (τ = 9 ns) (Visser & Lee, 1980). Its fluorescence lifetime can be shortened by the addition of the collisional quencher potassium iodide. The amount of potassium iodide was such that the viscosity was not altered. Figure 5 presents examples of deconvoluted anisotropy decay of lumazine at 20 and 3 °C. The results have been incorporated in Table I both for quenched and for unquenched fluorescence, and it is clear that both correlation times are similar, as expected. At lower temperature the correlation times were longer, mainly due to the higher viscosity of the aqueous solution (Table I). It should be noted that, for successful deconvolution, the time increment per channel must be chosen shorter than the shortest lifetime component in both fluorescence and anisotropy decay. One is then able to recover correlation times in the order of 100 ps from the experimental data. We also see in Figure 5 that the initial anisotropy is lower than the true one. This is due to the deconvolution, and from simulation studies such a decrease can be demonstrated (Papenhuyzen & Visser, 1983). Figure 6 presents two examples of such simulations. A Gaussian pulse profile of 0.5 ns completely overlaps the anisotropy decay curve with a correlation time of 100 ps (Figure 6A). Also significant is the lower initial anisotropy value (at t = 0 ns); a similar result is found experimentally. If the correlation time becomes longer, ϕ =

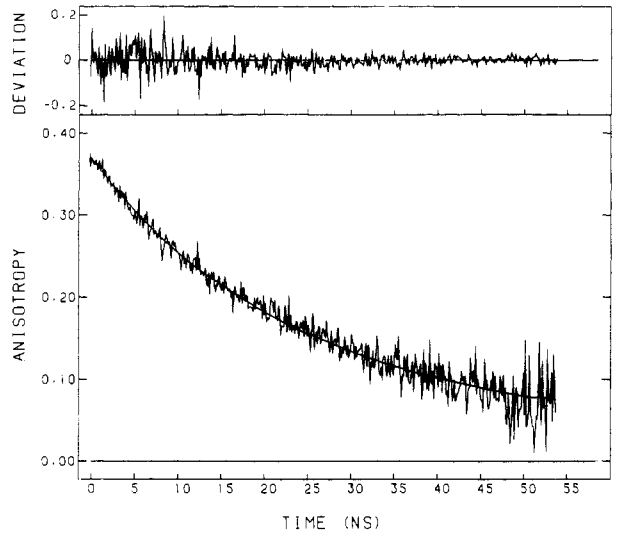

FIGURE 4: Anisotropy decay of 7.5 μM lumazine protein from *P. leiognathi* in the presence of 62 μM luciferase from *P. phosphoreum* in 1 M potassium phosphate, pH 7.0 at 2 °C. Experimental decay was fitted to a biexponential function with parameters $\beta_1 = 0.25$, $\phi_1 = 20$ ns, $\beta_2 = 0.13$, and $\phi_2 = 60$ ns; ϕ_1 and ϕ_2 were fixed during analysis (cf. Table II).

200 ps (Figure 6B), the $r(0)$ value rises. Shortening of the lifetimes from 9 to 1 ns has no effect at all on the true and apparent anisotropy decays, because the much shorter correlation time remains determining.

Discussion

With the test system consisting of the lumazine fluorophore free and bound to the apoprotein we have shown that anisotropy decays can be obtained with high precision and sensitivity. Both short (>100 ps) and long correlation times (10–100 ns) can be determined. As it should be, the correlation times obtained are independent of the fluorescence lifetimes. The measurement of biexponential decay and the associated recovery of the parameters have been shown to be feasible. Conditions were chosen such that the transition moments of absorption and emission of the chromophore can be considered to be identical, because of the red-edge excitation employed.

With the lumazine derivative tightly associated (the dissociation constant is 16 nM at 20 °C; Lee et al., 1985) one can expect that the initially photoselected molecular distribution gives rise to the limiting anisotropy of 0.4. We have found a small contribution of a very rapidly relaxing component in the anisotropy decay of the lumazine protein under conditions where the prosthetic group is completely bound (Lee et al., 1985). The observation of the rapid phenomenon depends on whether part of the pulse profile is included or not in the analysis. Such an effect must be ascribed to picosecond torsional vibrations of the molecule causing an instantaneous depolarization (Jablonski, 1965). We have also seen such rapid depolarization in several flavoproteins (unpublished observations). If a solution of a lumazine protein from the related bacterium *P. phosphoreum* is diluted, the lumazine ligand is released from the protein because the dissociation constant is much higher than the one for the *P. leiognathi* protein (Visser & Lee, 1980). This is manifested by a very rapid subnanosecond anisotropy decay (due to rotation of the free lumazine derivative) superimposed on the much slower decay attributable to protein rotational diffusion. This initial depolarization is due to rotation of a small molecule and should be distinguished from the depolarizing internal oscillation mentioned above. At this point we should make an important

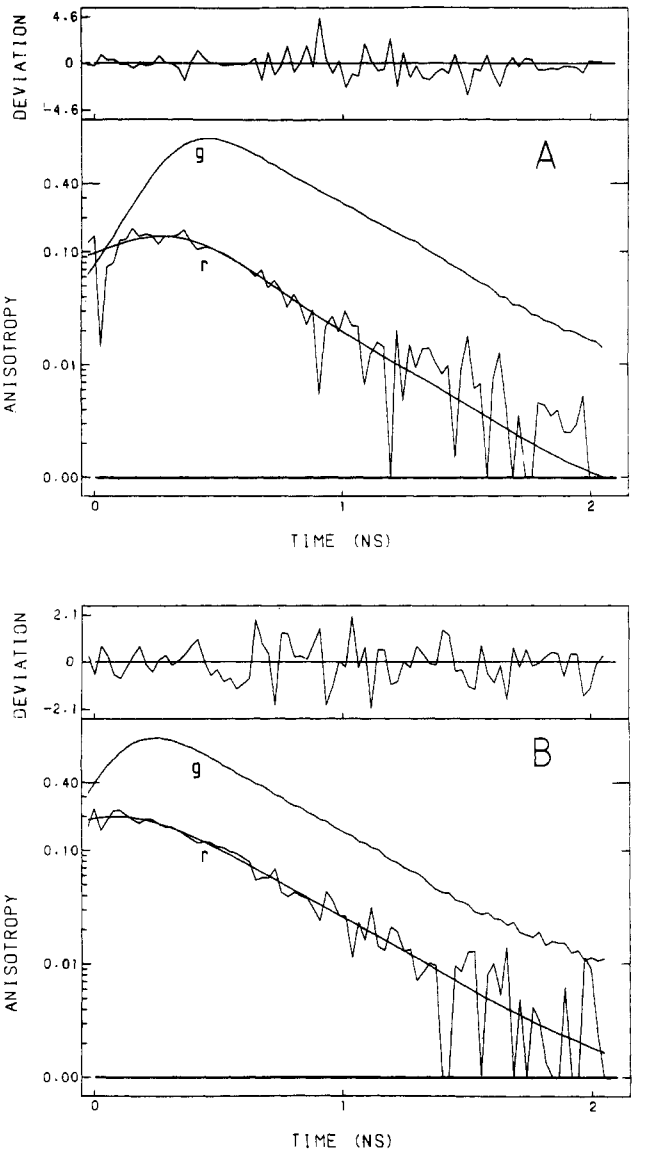

FIGURE 5: Anisotropy decay of free lumazine in aqueous phosphate buffer (0.05 M, pH 7.0) at 20 °C (A) and at 3 °C (B). The pulse profile has been incorporated in the figure to show that rigorous deconvolution is required to recover the picosecond correlation times: $\phi = 83$ ps at 20 °C, and $\phi = 157$ ps at 3 °C.

remark concerning the execution of the measurements. If the rapid component is to be resolved from the remainder of the decay, one should take care of an appropriate time equivalence per channel, i.e., much shorter than the shortest component of either fluorescence or anisotropy decay.

Inasmuch as the anisotropy decays according to a single exponential function, the correlation time obtained is that of spherical protein of nearly 30 kDa, while the anhydrous molecular mass has been determined to be 21 kDa (O'Kane & Lee, 1985b). A 21-kDa globular protein should give rise to a significantly shorter correlation time than obtained (6 ns instead of 9.5 ns at 20 °C) (Visser & Lee, 1982). The discrepancy is accounted for by the hydration of the protein (O'Kane & Lee, 1985b), which yields a much larger rotating particle. Also, the shape of the protein might deviate from a sphere, causing it to rotate slower, e.g., like a prolate ellipsoid. Since the composite correlation time of that situation would depend on the angle that the transition moment makes with the main symmetry axis of the ellipsoid (Berkhout et al., 1984), a demonstration of the effect might consist of replacing the natural fluorophore by another, closely related analogue. Such

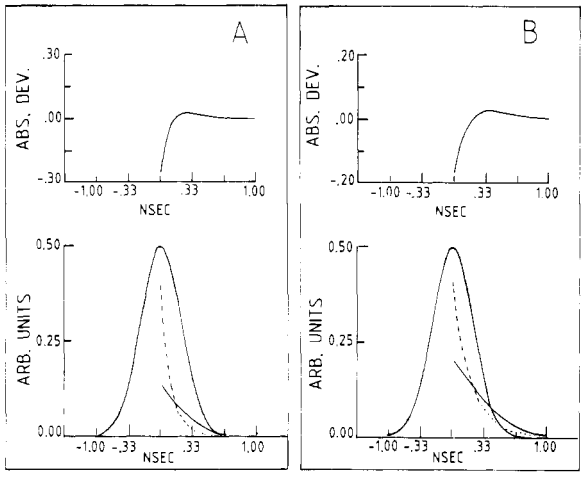

FIGURE 6: Simulated anisotropy decay. Shown are a 0.5-ns Gaussian excitation pulse response function (—) and the true (---) and apparent (—) anisotropy decay. (A) Simulation for τ = 9 ns and ϕ = 100 ps. (B) τ = 9 ns and ϕ = 200 ps. Note that the initial apparent decay (at t = 0 ns) is lower than the true one [$r(0)$ = 0.4] and also that the anisotropy decays within the pulse profile. A reduction of τ from 9 to 1 ns had virtually no effect on the apparent anisotropy decay profiles.

a compound should be similarly accommodated in the binding region of the protein, but with its dipole moment differently oriented in the molecular framework. Experiments are planned in the near future.

The strength of the protein–protein association experiments is their directness leading to a dissociation constant describing the binding behavior from a single experiment. Given the very large sensitivity of fluorescence, it is evident that anisotropy decay analysis is a powerful tool to investigate protein–protein association equilibria at nanomolar–micromolar concentrations. It is prerequisite that the lifetime of the complex (before it breaks apart) is much longer than the average fluorescence lifetime. We can also conclude that no significant shape changes occur upon complexation of lumazine protein with luciferase, since the longer correlation time is characteristic for a spherical particle of M_r 100 000.

Lumazine itself is quite a polar molecule; the calculated dipole moment in the ground state is of the order of 4 D (Platenkamp, 1981). In a strict sense the molecule should be considered as an anisotropic rotor; for instance, the aromatic part of the molecule may be assumed to be an oblate ellipsoid. This is important to note because in the absence of solute–solvent interactions rotational diffusion can be described on the assumption of slip boundary conditions (Fleming et al., 1976). This means that for such a molecule solvent must be displaced and the solvent cannot be considered as a continuous, noninteracting fluid. The large dipole moment, on the other hand, would imply a strongly solvated molecule, which rotates apparently in an isotropic fashion. This is the stick boundary condition in which the layer of fluid adjacent to the molecule moves at the same velocity. In this case the Stokes–Einstein relation holds true with radius R approximating half of the longest axis of the chromophore. Ignoring the size of the ribityl side chain, we calculated for the aromatic moiety, with R = 3.2 Å, ϕ = 300 ps at 20 °C. We have observed significantly shorter correlation times, which suggests that the molecule is indeed an oblate rotor. It was shown by Fleming et al. (1976) by numerical analysis that the decay law for such a case would closely resemble a single exponential when the transition moment is perpendicular to the main symmetry axis. The two rate constants arising from that model can be expressed in the two diffusion coefficients and the axial ratio of the oblate. It can be easily shown that for any value of the axial ratio the two diffusion constants have comparable values. If we assume the aromatic part of the lumazine molecule to be an oblate ellipsoid with semiaxes of 4 and 2 Å (the long axis is a little overestimated), the two reciprocal rate constants are calculated to be 37 and 43 ps, respectively, which indeed nearly correspond to a single correlation time of around 40 ps (20 °C). This is a lower bound value, since the measured correlation times are about 70–80 ps. Both the ribityl side chain and bound water molecules make the effective volume distinctly larger. Water has been shown to form an integral part of the lumazine molecule in its crystal structure (Norrestam et al., 1972).

To investigate the latter problem in more depth, one should really improve the time resolution up to the picosecond range, e.g., via up-conversion techniques (Beddard et al., 1981). Such improved time resolution is also required to register the rapid (picosecond) tryptophan motions in proteins, as recently demonstrated in lysozyme by molecular dynamics calculations (Ichiye & Karplus, 1983).

Registry No. KI, 7681-11-0; 6,7-dimethyl-8-ribityllumazine, 5118-16-1.

REFERENCES

Beddard, G., Doust, T. A. M., & Porter, G. (1981) *Chem. Phys. 61*, 17–23.

Belford, G. G., Belford, R. L., & Weber, G. (1972) *Proc. Natl. Acad. Sci. U.S.A. 69*, 1392–1393.

Berkhout, T., Visser, A. J. W. G., & Wirtz, K. W. A. (1984) *Biochemistry 23*, 1505–1513.

Dale, R. E. (1983) in *Time-Resolved Fluorescence Spectroscopy in Biochemistry and Biology* (Cundall, R. B., & Dale, R. E., Eds.) pp 555–612, Plenum Press, London.

Dale, R. E., Chen, L. A., & Brand, L. (1977) *J. Biol. Chem. 252*, 7500–7510.

Fleming, G. R., Morris, J. M., & Robinson, G. W. (1976) *Chem. Phys. 17*, 91–100.

Gafni, A., Modlin, R. L., & Brand, L. (1975) *Biophys. J. 15*, 263–280.

Grinvald, A., & Steinberg, I. Z. (1974) *Anal. Biochem. 59*, 583–598.

Haehnel, W., Nairn, J. A., Reisberg, P., & Sauer, K. (1982) *Biochim. Biophys. Acta 680*, 161–173.

Harris, Ch. M., & Selinger, B. K. (1979) *Aust. J. Chem. 32*, 2111–2129.

Harvey, S. C., & Cheung, H. C. (1980) *Biopolymers 19*, 913–930.

Heyn, M. P. (1979) *FEBS Lett. 108*, 359–364.

Ichiye, T., & Karplus, M. (1983) *Biochemistry 22*, 2884–2893.

Jablonski, A. (1965) *Acta Phys. Pol. 28*, 717–728.

Kinosita, K., Kawato, S., & Ikegami, A. (1977) *Biophys. J. 20*, 289–305.

Kinosita, K., Ikegami, A., & Kawato, S. (1982) *Biophys. J. 37*, 461–464.

Lampert, R. A., Chewter, L. A., Phillips, D., O'Connor, D. V., Roberts, A. J., & Meech, S. R. (1983) *Anal. Chem. 55*, 68–73.

Lee, J. (1982) *Photochem. Photobiol. 36*, 689–697.

Lee, J., Carreira, L. A., Gast, R., Irwin, R. M., Koka, P., Small, E. D., & Visser, A. J. W. G. (1981) in *Bioluminescence and Chemiluminescence* (DeLuca, M., & McElroy, W. D., Eds.) pp 103–112, Academic Press, New York.

Lee, J., O'Kane, D. J., & Visser, A. J. W. G. (1985) *Biochemistry* (third of five papers in this issue).

Lipari, G., & Szabo, A. (1980) *Biophys. J. 30*, 489–506.

Marquardt, D. W. (1963) *J. Soc. Ind. Appl. Math. 11*, 431-441.
McKinnon, A. E., Szabo, A. G., & Miller, D. R. (1977) *J. Phys. Chem. 81*, 1564-1570.
Munro, I., Pecht, I., & Stryer, L. (1979) *Proc. Natl. Acad. Sci. U.S.A. 76*, 56-60.
Norrestam, R., Stensland, B., & Söderberg, E. (1972) *Acta Crystallogr., Sect. B B28*, 659-666.
O'Connor, D. V., Ware, W. R., & Andre, J. C. (1979) *J. Phys. Chem. 83*, 1333-1343.
O'Kane, D. J., & Lee, J. (1985a) *Biochemistry* (second of five papers in this issue).
O'Kane, D. J., & Lee, J. (1985b) *Biochemistry* (fourth of five papers in this issue).
O'Kane, D. J., Karle, V. A., & Lee, J. (1985) *Biochemistry* (first of five papers in this issue).
Papenhuyzen, J., & Visser, A. J. W. G. (1983) *Biophys. Chem. 17*, 57-65.
Platenkamp, R. J. (1981) Ph.D. Thesis, Chapter 6, University of Leyden, The Netherlands.
Rigler, R., & Ehrenberg, M. (1973) *Q. Rev. Biophys. 6*, 139-199.
Searle, G. F. W., van Hoek, A., & Schaafsma, T. J. (1983) in *Picosecond Chemistry and Biology* (Doust, T. A. M., & West, M. A., Eds.) pp 35-67, Science Reviews Ltd., Northwood, Middlesex, England.
Small, E. D., Koka, P., & Lee, J. (1980) *J. Biol. Chem. 255*, 8804-8810.
Small, E. W., & Isenberg, I. (1977) *Biopolymers 16*, 1907-1928.
Tao, T. (1969) *Biopolymers 8*, 609-632.
Thomas, J. C., Allison, S. A., Appellof, C. J., & Schurr, J. M. (1980) *Biophys. Chem. 12*, 177-188.
Turko, B. T., Nairn, J. A., & Sauer, K. (1983) *Rev. Sci. Instrum. 54*, 118-120.
van Hoek, A., & Visser, A. J. W. G. (1981) *Rev. Sci. Instrum. 52*, 1199-1205.
van Hoek, A., & Visser, A. J. W. G. (1983) *Rev. Sci. Instrum. 54*, 1145-1147.
van Hoek, A., Vervoort, J., & Visser, A. J. W. G. (1983) *J. Biochem. Biophys. Methods 7*, 243-254.
Vervoort, J., O'Kane, D. J., Carreira, L. A., & Lee, J. (1983) *Photochem. Photobiol. 37*, 117-119.
Visser, A. J. W. G., & van Hoek, A. (1979) *J. Biochem. Biophys. Methods 1*, 195-208.
Visser, A. J. W. G., & Lee, J. (1980) *Biochemistry 19*, 4366-4372.
Visser, A. J. W. G., & van Hoek, A. (1981) *Photochem. Photobiol. 33*, 35-40.
Visser, A. J. W. G., & Lee, J. (1982) *Biochemistry 21*, 2218-2226.
Wahl, Ph. (1977) *Chem. Phys. 22*, 245-256.
Wahl, Ph. (1979) *Biophys. Chem. 10*, 91-104.
Wahl, Ph. (1983) in *Time-Resolved Fluorescence Spectroscopy in Biochemistry and Biology* (Cundall, R. B., & Dale, R. E., Eds.) pp 497-521, Plenum Press, London.
Yguerabide, J. (1972) *Methods Enzymol. 26C*, 498-578.
Yguerabide, J., Epstein, H. F., & Stryer, L. (1970) *J. Mol. Biol. 51*, 573-590.

The Histidine-Rich Glycoprotein of Serum Has a Domain Rich in Histidine, Proline, and Glycine That Binds Heme and Metals†

William T. Morgan
Department of Biochemistry, Louisiana State University Medical Center, New Orleans, Louisiana 70112
Received July 13, 1984

ABSTRACT: Histidine-rich glycoprotein (HRG) from rabbit serum was digested with plasmin, reduced, and carboxymethylated, and the fragments produced were resolved by reverse-phase high-performance liquid chromatography. Several peptide fractions were obtained that contain unusually high contents of histidine, proline, and glycine. One His-Pro-Gly-rich peptide (apparent M_r 30 000) was obtained in sufficient yield and purity for further study. This peptide is 29 mol % histidine, 37% proline, and 16% glycine, indicating that most of these three amino acids are located in one region of HRG. The peptide contains 9% by weight carbohydrate and is devoid of tyrosine or tryptophan. The far-ultraviolet circular dichroism spectrum of the peptide has a minimum at 203 nm, indicating that the peptide contains polyproline II helical sections. The peptide represents a binding domain of HRG since it retains much of the ability of intact HRG to bind heme and metals including Zn^{2+}, Ni^{2+}, and Cu^{2+}. As with the parent HRG molecule, interaction of the peptide with heme and metals is dependent on pH and intact histidine residues.

The histidine-rich glycoprotein[1] (HRG) of serum presents an interesting subject for protein structure–function studies. This protein has been isolated and characterized from both human (Heimburger et al., 1972; Morgan, 1978) and rabbit (Morgan, 1981) serum. In both cases, the protein has a single polypeptide chain, contains a fairly high amount of carbohydrate (ca. 15%), and has an unusually high content of proline as well as histidine. As a first step in determining the structure of this protein, an examination of the arrangement of these

† This work was supported in part by a grant from the USPHS, National Institutes of Health (HD 14481).

[1] Abbreviations: HRG, histidine-rich glycoprotein; heme, iron protoporphyrin IX; mesoheme, iron mesoporphyrin IX; $NaDodSO_4$, sodium dodecyl sulfate; Me_2SO, dimethyl sulfoxide; TFA, trifluoroacetic acid; EDTA, ethylenediaminetetraacetic acid; HPLC, high-performance liquid chromatography; RCM, reduced and carboxymethylated; Hepes, *N*-(2-hydroxyethyl)piperazine-*N'*-2-ethanesulfonic acid.

0006-2960/85/0424-1496$01.50/0